Design Principles for Block Polymer Organic Double Heterojunction Solar Cells

SCHOLARONE™
Manuscripts

Journal Name

ARTICLE

Design Principles for Block Polymer Organic Double Heterojunction Solar Cells

M. P. J. Hutnan[a] and L. G. Kaake[a]

An organic double heterojunction photovoltaic device is described and the limits of its power conversion efficiency are investigated via numerical calculation. In the absence of exciton binding energy, fully conjugated block polymer devices exhibit power conversion efficiencies slightly exceeding the Shockley-Queissar limit. As exciton binding energy increases, a decrease in efficiency occurs, but remains over 20% for binding energies less than 0.5 eV. Further calculations show that devices require a high degrees of phase purity to leverage the full benefit of the double heterjunction structure. Synthetic targets are identified and their maximum efficiency is calculated based on experimentally measured energy levels, leading to a generalized structural motif.

Introduction

Polymers and molecular solids are well known for their ability to harvest solar energy, and offer the promise of inexpensive photovoltaic devices which use earth abundant and non-toxic elements.[1,2] Currently, this technology is well-suited to serve the market with flexible and building integrated solar panels. In order to make organic solar cells a dominant technology useful for a multitude of applications, innovations to cell design must be made that bring devices closer to the Shockley-Queissar limit.[3] For this reason, three component cells have received considerable attention recently, and improvements in device efficiency over two component cells indicate the promise of this approach.[4] However, we believe that the full potential of a three component organic solar cell has yet to be realized and carefully articulated design principles are critical to this end. Here, we present a selective perspective on bulk heterojunction photophysics in order to suggest a three component cell design that takes advantage of and amplifies ultrafast charge and energy transport. In particular, we propose a double heterojunction structure and demonstrate that radically improved power conversion efficiencies are possible with this design.

It is desirable to improve the absorption characteristics of the cell through the introduction of non-fullerene acceptors[5] and much of the effort into three component organic solar cells has focused on this aspect of device design.[4] However, the biggest challenge to dramatically increasing power conversion efficiency in already high-performing organic photovoltaic materials is to increase the open-circuit voltage (V_{OC}) without compromising the current at short circuit (J_{SC}) and device fill-factor (FF).

To design such a cell, we draw the ionization potential (IP) and electron affinity (EA) of several species involved in photocurrent production within a bulk heterojunction (see figure 1). This energy level representation was chosen because it balances photophysical rigor with insight into the important energy levels which determine device function.[6] For example, Fig. 1 illustrates exciton binding energy (E_B) as the difference between the electron affinity of the ground state (EA_{S0}) and the ionization potential of the singlet exciton (IP_{S1}). This is the energy required to convert a fully relaxed exciton into a mobile charge carrier. In many electron donor materials $E_B^D = IP_{S1}^D - EA_{S0}^D$ is 300 meV or greater, although experiments on high performance molecular donor materials provide evidence of very low exciton binding energies.[7,8]

The energetic driving force for electron transfer in a solar cell is the difference in the ionization potential of the singlet exciton in the electron donor (IP_{S1}^D) minus the electron affinity of the ground state of the electron acceptor (EA_{S0}^A). Evidence is mounting that electron transfer is efficient even for small energy offsets,[9-12] meaning that the primary function of a large energy offset is to
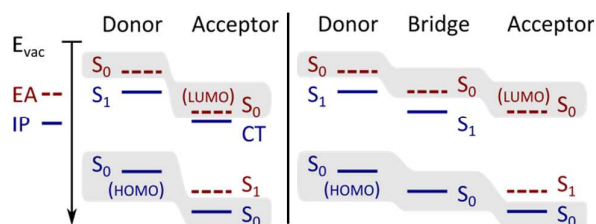

Fig 1. Schematic energy level diagram of organic solar cell components.

[a.] Department of Chemistry, Simon Fraser University, Burnaby, British Columbia, Canada V5A 1S6.

hinder bimolecular recombination of electrons and holes through low lying triplet states.[13]

Although energetic offsets at the D/A interface are necessary to avoid recombination and produce long-lived mobile carriers, it does so at the cost of reducing V_{OC}. The ground state of the charge transfer exciton is the primary determinant of V_{OC}[14] in the absence of impurity-enhanced recombination[15,16] or large contact resistance. This conclusion follows naturally from considerations of detailed balance.[17] The cell behaves like an indirect gap semiconductor, maintaining an absorption onset at greater energy than eV_{OC}. As a result, the single-junction Shockely-Quiessar limit cannot be approached.

In order to increase power conversion efficiency, the energy of the charge-transfer exciton state that determines V_{OC} must be increased. Figure 1 illustrates a double heterojunction device architecture which may accomplish this task. A third material, called the bridge, is inserted between the electron donor and the electron acceptor such that all charge carriers must traverse the bridge to move between the electron donor and the electron acceptor. The primary advantage of this configuration is the elimination of the CT exciton across the donor-acceptor interface. Instead, bimolecular charge recombination is forced to occur across the bridge, providing a synthetic handle for increasing V_{OC}.

The donor-bridge-acceptor molecular configuration is a cornerstone of electron transfer research.[18,19] However, this familiar configuration is better termed a "donor-barrier-acceptor" system in the context of organic double heterojunction solar cells. The energy levels of the "barrier" in familiar electron transfer studies are set such that they decrease charge transfer rates rather than acting a conduit for electron conduction. Although the "donor-barrier-acceptor" configuration can be used to make working photovoltaic cells,[20-29] it is not the primary focus of this work. Specifically, the ideal double heterojunction described here places the energy of the bridge in resonance with the energy of the molecular photoexcitation, (e.g. $EA_{S0}^B = IP_{S1}^D$ or $IP_{S0}^B = EA_{S1}^A$) and requires unbroken conjugation[30] to facilitate ultrafast charge separation. To restate, the double heterojunction solar cell described here relies on fast and thermodynamically favourable electron transfer process into the bridge to ensure efficient charge generation.

Calculations

In order to clearly describe the challenges and benefits of this solar cell design, a detailed balance model for the electrical characteristics of an ideal double heterojunction solar cell was constructed. A detailed description of the model can be found in the supporting information. Briefly, the voltage dependent solar cell current was calculated as the

difference between the dark current and the current resulting from charge photogeneration (J_G). Two components of the dark current were considered. Diode current across the bridge (J_{diode}) is the primary source of radiative recombination,[31,32] and non-radiative recombination as the result of tunnelling (J_{tunnel}) across the bridge. The latter is comprised of both tunnelling though a rectangular barrier and Fowler-Nordheim tunnelling mechanisms. Both are required to describe a wide range of voltages and wire lengths.[33]

$$J(V) = -J_G(V) + J_{diode}(V) + J_{tunnel}(V)$$

In the simplest case, the charge generation current can be calculated from by considering the balance of solar radiation (we used the AM 1.5 solar spectrum) and the blackbody emission of the cell. This treatment assumes the material is a perfect, voltage independent absorber of all radiation with energies greater than its optical gap. In the case of the DBA cell described here, the donor and the acceptor were considered perfect absorbers at short circuit. However, near the open circuit voltage, a large number of charge carriers can accumulate in the donor and acceptor regions of the cell as the quasi-Fermi level approaches the transport level of either material. Changing the charge state of a polymer or molecule changes its ability to absorb light, rendering it largely transparent in the visible region of the spectrum.[34] Moreover, the absorptions that appear (as dictated by sum rules) are typically incapable of producing photovoltaic currents. Thus, the absorption events that contribute to photocurrent decrease with voltage and are modelled by subtracting the voltage-dependent thermal distribution of charged molecules.[31]

The quantum efficiency of the charge generation process is modelled by considering two factors. First, the electron (or hole) transfer process must be thermodynamically favourable, assigning unit probability in those cases and zero probability if the electron transfer process is endothermic. Although electron transfer processes can occur through the bridge via a tunnelling mechanism, if the bridge energy is higher than the molecular exciton, this type of solar cell has been studied,[35] and is not the subject of this work. The second consideration governing the efficiency of the charge generation process applies to the length of the bridge; charges must traverse the bridge prior to a geminate recombination event. Recent reports illustrate that ultrafast charge transfer results in electron and hole separations of several nanometres in bulk heterojunction materials.[36] Further research is required to clarify the exact relationship between bridge length and charge separation efficiency but 5 nm will be taken as an upper bound of bridge lengths capable of producing charges with unit efficiency.

Results and discussion

Materials Horizons

The power conversion efficiency of ideal DBA solar cells in the absence of exciton binding energy is displayed in fig. 2a. In this calculation we set the optical gap of the donor, $E_G(D)$, equal to that of the acceptor, $E_G(A)$, and allowed that gap to vary independently of the optical gap of the bridge, $E_G(B)$. The highest efficiencies were achieved with $E_G(D) = E_G(A)$ as the cells are already assumed to absorb all incident light. The relative positions of the energy levels were assigned by setting the singlet exciton state of the donor, $IP_{S1}(D)$, equal to the electron affinity of the bridge, $EA_{S0}(B)$. This condition is the limit of small thermodynamic driving force for electron transfer into the bridge. If this condition is sufficient for highly efficient electron transfer, it represents an upper bound on device efficiency. Similar considerations were applied to the complementary hole transfer process, namely, the electron affinity of the singlet exciton state of the acceptor $EA_{S1}(A)$ was set equal to the ionization potential of the bridge $IP_{S0}(A)$.

The upper left half of fig. 2a shows a peak near the diagonal while the lower right half of the graph is a region with energetically unfavourable charge transfer reactions. Device efficiencies for the latter were not calculated. To more clearly display the relationship between the optical gap of the solar cell and ultimate device efficiency, fig. 2b shows diagonal slices taken from Fig. 2a. Two slices are of particular interest. The case where $E_G(D) = E_G(B) = E_G(A)$ represents an ideal P-N junction and accordingly, the Shockley-Queissar limit is obtained. The diagonal slice containing the highest efficiency from fig. 2a occurs when $E_G(D) = E_G(A)$ and $E_G(B) = E_G(D) + 0.1\ eV$. The net result is an energetic offset of 0.05 eV between the donor and the acceptor; this improves the efficiency primarily by increasing the quality of the diode. In other words, the offset reduces the number of carriers with sufficient energy to participate in the recombination reactions that drive the diode current. This effect is not dissimilar from that of a P-N junction operating at lower temperature (see fig. 2b) and is consistent with reports that organic solar cells can have fill factors above the Shockley-Queissar limit.[37]

Figs. 2c and 2d show the different contributions to the current for a cell of $E_G(D) = E_G(A) = 1.25$ and $E_G(B) = 1.35$. Note the roll-off of the current generation at high reverse bias as a result of highly populated transport levels. Additionally, the contributions to the recombination current, plotted on a logarithmic scale, show that the tunnelling currents in this configuration are minor. Thus, the parameters used are representative of the upper bound of double heterojunction device efficiencies.

That a double heterojunction allows for efficiencies slightly higher than the Shockley-Queissar limit should not surprise; it is more complicated than a single P-N junction. The small gain in efficiency relative to the increased complexity makes this strategy unattractive for highly ordered inorganic materials. However, and most importantly, the real utility of the double heterojunction cell is for excitonic materials.

Fig. 3 demonstrates the effect of increasing exciton binding energy on device efficiency and was calculated assuming all materials possess the same exciton binding energy. When including
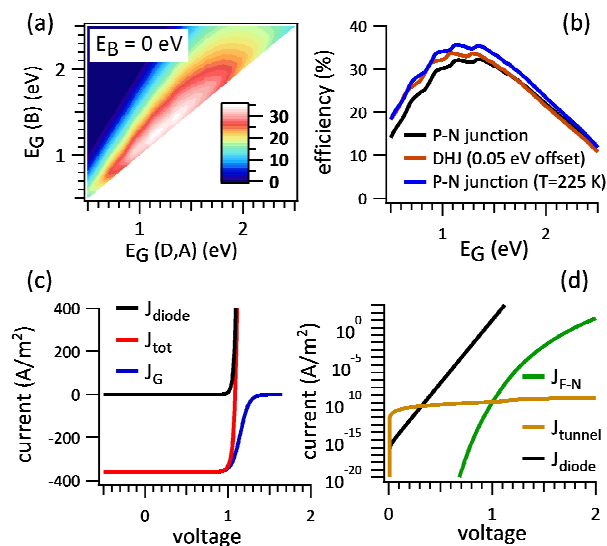

Fig. 2 Calculated solar cell parameters in the absence of exciton binding energy. (a) Power conversion efficiency for double heterojunction device as a function of energy gap of bridge versus donor and acceptor. (b) Power conversion efficiency for cells described in the text. (c,d) Current-voltage behaviour of champion double heterojunction cell.

exciton binding energy in the bridge, it is critical to avoid Förster energy transfer into the bridge. If the bridge possesses a non-zero exciton binding energy, charge transfer reactions are not guaranteed to be energetically favourable, and the exciton will not contribute to photocurrent. As a result of enforcing this energetic requirement, an overall decrease in device efficiency is observed in the presence of stronger exciton binding energy. The efficiency maximum of the double heterojunction cell shifts towards higher optical gaps to compensate for the exciton binding energy, moving
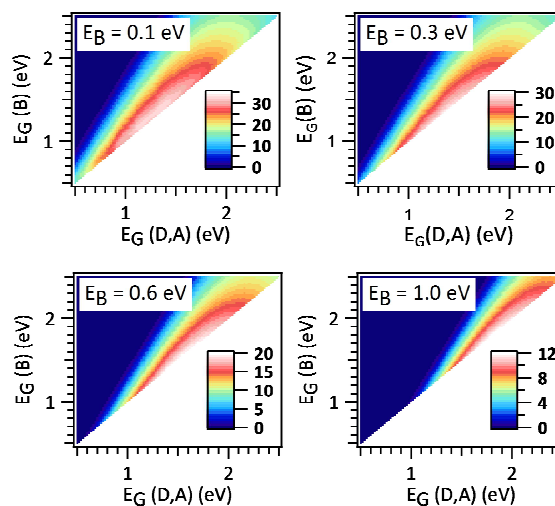

Fig. 3 Calculated power conversion efficiency for double heterojunction cells with different exciton binding energies (E_B).

it away from the ideal P-N junction and into a parameter space of lower efficiency, in accord with the predictions of Forrest and co-workers.[38] As shown in the supporting information, the primary reason the double heterojunction outperforms the standard donor-acceptor configuration is that the double heterojunction cell can maintain a large V_{OC} in the presence of non-zero exciton binding energies.

To obtain the full benefits of the double heterojunction cell configuration, it is important that all recombination occur through the bridge. This emphasis differentiates the double heterojunction concept from the ternary blend or cascaded energy structure. Having all recombination occur through the bridge cannot be accomplished in the presence of direct donor-acceptor contacts. This places stringent constraints on the purity of the donor and acceptor phases. This effect was modelled by placing donor-acceptor cells in parallel with double heterojunction cells and characterizing the result according to the fraction of donor-acceptor solar cells (f_{DA}) relative to the total. Donor-acceptor cells are conveniently modelled within the computational framework presented here by using the bridge state to represent the charge transfer exciton. The ground state electron affinity and ionization potential of the charge transfer exciton $\left(EA_{SO}(CT), IP_{SO}(CT)\right)$ are purely theoretical quantities, but the singlet exciton states can be defined relative to them by adding the exciton binding energy. To model the charge transfer exciton energies, we set $EA_{SO}(CT) = EA_{SO}(A)$ and $IP_{SO}(CT) = IP_{SO}(D)$, resulting in the energy level diagram shown in Fig. 4a. Calculated device efficiencies are shown in Fig. 4b for a pure donor-acceptor solar cell using an exciton binding energy of 0.3 eV. In this figure, $E_G(B)$ is to be understood as a quantity related to the energy offset at the donor-acceptor
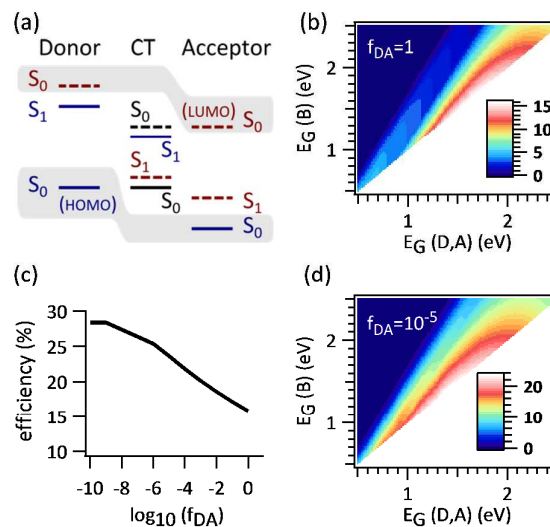

Fig. 4 Effects of direct donor-acceptor contacts. (a) Energy level diagram of donor-acceptor model. (b,d) Power conversion efficiency as a function of optical gap. (c) Maximum cell efficiency versus fraction of donor-acceptor contacts.

interface. Specifically, the offset is half of the difference between $E_G(B)$ and $E_G(D, A)$.

Fig. 4c shows how the maximum possible device efficiency is affected by the presence of donor-acceptor contacts, nearly doubling from a pure donor-acceptor cell (f_{DA} = 1) to a pure double heterojunction cell ($f_{DA} \rightarrow 0$). As Fig. 5c shows, direct DA contacts are to be scrupulously avoided; obtaining most of the benefit of the double heterojunction requires phase purity at ppm levels. This
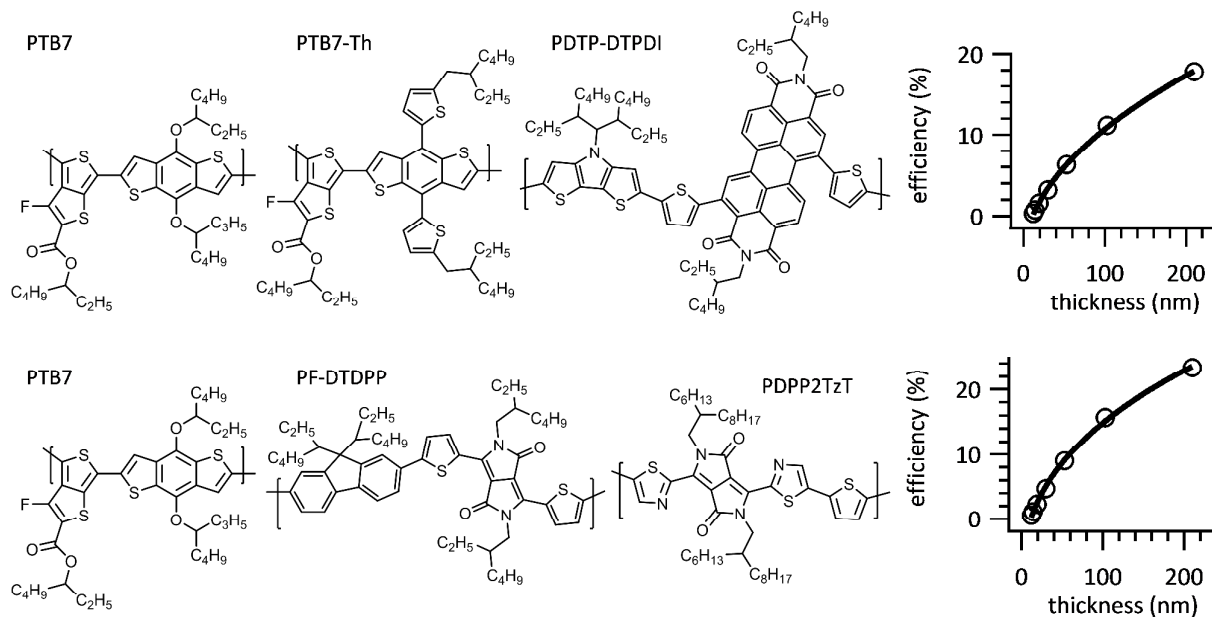

Fig. 5 Examples of double heterojunction triblock polymers. Components are listed in donor-bridge-acceptor order, from left to right. Calculated cell efficiencies as a function of active layer thickness for each example is given beside it.

calculation demonstrates that the current generation of three component systems,[4] which often do not carefully control phase purity, could be significantly and dramatically improved. Although it is high, the required phase purity may be possible to achieve in copolymer systems, where demixing of polymer phases is thermodynamically favourable.[39] In fact, the requirements for phase purity present a compelling rationale for a block polymer configuration. It seems unlikely that oligomers or copolymers can simultaneously support a bicontinuous percolating network of donor and acceptor phases while maintaining phase purity at the ppm level. Finally, fig. 4d shows how the double heterojunction cell favors lower optical gaps; the maximum shifts down and to the left when the number of donor-acceptor contacts is reduced from f_{DA} =1 to f_{DA} =10^{-4}.

Finally, we performed a literature search to identify promising double heterojunction systems, and provide a testable, quantitative prediction of our calculations. The first system uses PTB7[40] as the donor, PTB7-Th[41] as the bridge and PDTP-PTPDI[42] as the acceptor. (See fig. 5 for molecular structures) The second system uses PTB7[40] as the donor, PC-DTDPP[43] as the bridge, and PDPP2TzT[44] as the acceptor. In the calculation, the cell comprised equal parts donor and acceptor, and the length of the bridge was taken as 5 nm. The efficiency of each cell was calculated using a identical method as described above using published energy levels. However, instead of assuming that all above gap radiation is absorbed, the calculation used published absorption spectra to estimate the wavelength dependent molar absorbtivity of the film.

Thickness dependent solar cell efficiencies for the two identified double heterojunction systems are provided in fig. 5. Both systems substantially outperform their analogous two-component cells. However, the synthetic complexity of each system is daunting to say the least. It is unclear at present whether the complexity of each unit is necessary for successful implementation into a double heterojunction cell. It is somewhat likely that a significant fraction of the molecular complexity evolved from the morphological complexity of the standard bulk heterojunction solar cell and it is possible that much of that complexity can be jettisoned when implementing a double heterojunction configuration.

The proposed systems also share an interesting feature; the bridge comprises structurally identical components to the donor or the acceptor. The LUMO level of the bridge should nearly align with the donor, and the HOMO level of the bridge should nearly align with the acceptor. In the current generation of "donor-acceptor" polymers, the LUMO is associated with the more electronegative portion of the polymer, while the HOMO is associated with the electron donating portion of the polymer. It is thus reasonable to suggest that a successful bridge material would comprise the more electronegative portion of the donor section of the double heterojunction and the deeper lying portion of the acceptor section. In symbols, we speculate that the preferred motif of a successful double heterojunction is as follows:

$$[D - A] - [D' - A] - [D' - A']$$

In this context, D and D' describe the less electronegative portion of a "donor-acceptor" polymer. Similarly, A and A' describe the more electronegative portion of a "donor-acceptor" polymer. This schematic provides a general description of how the cascading energy structure described here might be achieved.

Conclusions

An organic double heterojunction solar cell was proposed and its properties were investigated via numerical calculation. The results indicate that device efficiencies greater than 20% are possible in systems with exciton binding energies less than 0.6 eV. The preferred arrangement of the double heterojunction is an all-conjugated block polymer. The relationship between film morphology and device efficiency was investigated and suggests that phase purity is of primary importance in achieving highly efficient devices. Lastly, specific examples of a double heterojunction were given and their efficiencies were calculated to be greater than 15% for films of ~200 nm. Although the proposed systems appear extremely complex from a synthetic perspective, a generalized structural motif was proposed, which we hope can be used to develop a more synthetically tractable material.

Acknowledgements

Notes and references

1   C. W. Tang, *Applied Physics Letters*, 1986, **48**, 183-185.
2   G. Yu, J. Gao, J. C. Hummelen, F. Wudl and A. J. Heeger, *Science*, 1995, **270**, 1789-1791.
3   W. Shockley and H. J. Queisser, *Journal of Applied Physics*, 1961, **32**, 510-519.
4   P. Cheng and X. Zhan, *Materials Horizons*, 2015, **2**, 462-485.
5   S. M. McAfee, J. M. Topple, I. G. Hill and G. C. Welch, *Journal of Materials Chemistry A*, 2015, **3**, 16393-16408.
6   X. Y. Zhu, *J. Phys. Chem. Lett.*, 2014, **5**, 2283-2288.
7   J. J. Jasieniak, B. B. Y. Hsu, C. J. Takacs, G. C. Welch, G. C. Bazan, D. Moses and A. J. Heeger, *ACS Nano*, 2012, **6**, 8735-8745.
8   L. G. Kaake, J. J. Jasieniak, R. C. Bakus, G. C. Welch, D. Moses, G. C. Bazan and A. J. Heeger, *J. Am. Chem. Soc.*, 2012, **134**, 19828-19838.
9   G. Ren, C. W. Schlenker, E. Ahmed, S. Subramaniyan, S. Olthof, A. Kahn, D. S. Ginger and S. A. Jenekhe, *Advanced Functional Materials*, 2013, **23**, 1238-1249.
10   S. D. Oosterhout, N. Kopidakis, Z. R. Owczarczyk, W. A. Braunecker, R. E. Larsen, E. L. Ratcliff and D. C. Olson, *Journal of Materials Chemistry A*, 2015, **3**, 9777-9788.
11   R. D. Pensack and J. B. Asbury, *J. Am. Chem. Soc.*, 2009, **131**, 15986-15987.

12   B. F. Wright, K. Sunahara, A. Furube, A. Nattestad, T. M. Clarke, G. C. Bazan, J. D. Azoulay and A. J. Mozer, *J. Phys. Chem. C*, 2015, **119**, 12829-12837.

13   A. Rao, P. C. Y. Chow, S. Gelinas, C. W. Schlenker, C.-Z. Li, H.-L. Yip, A. K. Y. Jen, D. S. Ginger and R. H. Friend, *Nature*, 2013, **500**, 435-439.

14   K. Vandewal, K. Tvingstedt, A. Gadisa, O. Inganas and J. V. Manca, *Nat. Mater.*, 2009, **8**, 904-909.

15   S. R. Cowan, A. Roy and A. J. Heeger, *Physical Review B*, 2010, **82**, 245207.

16   L. Kaake, X. D. Dang, W. L. Leong, Y. Zhang, A. Heeger and T. Q. Nguyen, *Adv. Mater.*, 2013, **25**, 1706-1712.

17   U. Rau, *Physical Review B*, 2007, **76**, 085303.

18   M. R. Wasielewski, *Accounts Chem. Res.*, 2009, **42**, 1910-1921.

19   O. S. Wenger, *Accounts Chem. Res.*, 2011, **44**, 25-35.

20   S. S. Sun, C. Zhang, A. Ledbetter, S. Choi, K. Seo, C. E. Bonner, M. Drees and N. S. Sariciftci, *Applied Physics Letters*, 2007, **90**, 043117.

21   S. S. Sun, J. Brooks, T. Nguyen and C. Zhang, *J. Polym. Sci. Pol. Chem.*, 2014, **52**, 1149-1160.

22   C. Guo, Y.-H. Lin, M. D. Witman, K. A. Smith, C. Wang, A. Hexemer, J. Strzalka, E. D. Gomez and R. Verduzco, *Nano Letters*, 2013, **13**, 2957-2963.

23   N. Sary, F. Richard, C. Brochon, N. Leclerc, P. Leveque, J. N. Audinot, S. Berson, T. Heiser, G. Hadziioannou and R. Mezzenga, *Adv. Mater.*, 2010, **22**, 763-768.

24   Q. L. Zhang, A. Cirpan, T. P. Russell and T. Emrick, *Macromolecules*, 2009, **42**, 1079-1082.

25   Y. F. Tao, B. McCulloch, S. Kim and R. A. Segalman, *Soft Matter*, 2009, **5**, 4219-4230.

26   K. Sivula, Z. T. Ball, N. Watanabe and J. M. J. Frechet, *Adv. Mater.*, 2006, **18**, 206-210.

27   G. Hadziioannou, *Mrs Bulletin*, 2002, **27**, 456-460.

28   J. Wang, M. Ueda and T. Higashihara, *J. Polym. Sci. Pol. Chem.*, 2014, **52**, 1139-1148.

29   Y. H. Lin, K. G. Yager, B. Stewart and R. Verduzco, *Soft Matter*, 2014, **10**, 3817-3825.

30   S. Y. Ku, M. A. Brady, N. D. Treat, J. E. Cochran, M. J. Robb, E. J. Kramer, M. L. Chabinyc and C. J. Hawker, *J. Am. Chem. Soc.*, 2012, **134**, 16040-16046.

31   J. Nelson, *The Physics of Solar Cells*, Imperial College Press, 2003.

32   R. A. J. Janssen and J. Nelson, *Adv. Mater.*, 2013, **25**, 1847-1858.

33   S. Ho Choi, B. Kim and C. D. Frisbie, *Science*, 2008, **320**, 1482-1486.

34   A. J. Heeger, N. S. Sariciftci and E. B. Namdas, *Semiconducting and Metallic Polymers*, Oxford University Press, 2010.

35   F. L. Liu, B. K. Crone, P. P. Ruden and D. L. Smith, *Journal of Applied Physics*, 2013, **113**, 044516.

36   S. Gélinas, A. Rao, A. Kumar, S. L. Smith, A. W. Chin, J. Clark, T. S. van der Poll, G. C. Bazan and R. H. Friend, *Science*, 2014, **343**, 512-516.

37   V. A. Trukhanov, V. V. Bruevich and D. Y. Paraschuk, *Scientific Reports*, 2015, **5**, 11478.

38   N. C. Giebink, G. P. Wiederrecht, M. R. Wasielewski and S. R. Forrest, *Physical Review B*, 2011, **83**, 195326.

39   P. C. Hiemenz and T. P. Lodge, *Polymer Chemistry, Second Edition*, Taylor & Francis, 2007.

40   Y. Y. Liang, Z. Xu, J. B. Xia, S. T. Tsai, Y. Wu, G. Li, C. Ray and L. P. Yu, *Adv. Mater.*, 2010, **22**, E135–E138.

41   S. H. Liao, H. J. Jhuo, Y. S. Cheng and S. A. Chen, *Adv. Mater.*, 2013, **25**, 4766-4771.

42   E. Zhou, K. Tajima, C. H. Yang and K. Hashimoto, *J. Mater. Chem.*, 2010, **20**, 2362-2368.

43   E. J. Zhou, S. P. Yamakawa, K. Tajima, C. H. Yang and K. Hashimoto, *Chemistry of Materials*, 2009, **21**, 4055-4061.

44   W. W. Li, W. S. C. Roelofs, M. Turbiez, M. M. Wienk and R. A. J. Janssen, *Adv. Mater.*, 2014, **26**, 3304-3309.

Simon Fraser University
Department of Chemistry
8888 University Drive
Burnaby BC
Canada V5A 1S6
TEL 778.782.9915
lkaake@sfu.ca

Statement of Conceptual Insight

The continued vitality and relevance of organic photovoltaic research relies on improvements in device efficiency, stability, and manufacturability. This is especially important given the intense competition from other emerging materials classes. This work describes a new geometry for organic solar cells and demonstrates the theoretical limits of its power conversion efficiency. The double heterojunction geometry is predicted be more than double that of the bulk heterojunction. Moreover, the work describes several important design considerations and presents a generalized chemical structure to provide useful guidance to synthetic chemists interested in pursuing an organic double heterojunction device structure. The guidelines are sufficiently general to allow for the development of entire libraries of new materials. Should these materials function as described herein, organic photovoltaics would find significantly wider utility, emerging as a truly disruptive technology in solar energy conversion.

Sincerely,

Dr. Loren Kaake
Assistant Professor of Chemistry
Simon Fraser University